

SYNTHESIS, STRUCTURE, AND PROPERTIES OF POTASSIUM *fac*-TRICHLOROTRINITROIRIDATE(III)*

P. A. Topchiyan¹, V. A. Nikolaev²,
N. V. Kuratieva¹, D. B. Vasilchenko^{1**},
and S. V. Korenev¹

Potassium salt of the iridium(III) chloronitro complex *fac*-K₃[Ir(NO₂)₃Cl₃] is obtained in the interaction of the iridium(III) trinitrotrihydroxo complex with potassium chloride in an aqueous solution. The salt structure is analyzed by single crystal X-ray diffraction. Crystallographic data: $a = 7.3460(3) \text{ \AA}$, $b = 12.9904(5) \text{ \AA}$, $c = 13.1841(6) \text{ \AA}$, $\beta = 93.924(1)^\circ$, space group $P2_1/c$, $Z = 4$, $\rho_{\text{cal}} = 3.026 \text{ g/cm}^3$. In the crystal structure, molecules of the $[\text{Ir}(\text{NO}_2)_3\text{Cl}_3]^{3-}$ complex anion having a distorted octahedral geometry ($\text{Ir-N} = 2.02\text{--}2.04 \text{ \AA}$, $\text{Ir-Cl} = 2.37\text{--}2.38 \text{ \AA}$) are arranged in layers perpendicular to the c axis. Spectral characteristics (IR, Raman, UV-vis) of the salt are determined together with its transformations during thermolysis in the inert atmosphere. Experiments are performed on sorption of the $[\text{Ir}(\text{NO}_2)_3\text{Cl}_3]^{3-}$ complex on nickel hydroxide, which model iridium loss during the precious metal refining process by the precipitation scheme.

DOI: 10.1134/S0022476623070132

Keywords: iridium, nitro complexes, chloro complexes, aqua complexes, single crystal X-ray diffraction analysis, spectroscopy, sorption.

INTRODUCTION

Iridium(III) chloronitro complexes have been known as intermediate forms of iridium existence during nitration of hexachloroiridates in refining of platinum group metals (PGMs). In the course of separation of these metals, iridium, rhodium, and ruthenium chloro complexes transform into soluble salts of anionic nitro complexes $[\text{M}(\text{NO}_2)_6]^{3-}$ for Rh, Ir and $[\text{Ru}(\text{NO})(\text{NO}_2)_4(\text{OH})]^{2-}$, with accompanying non-precious metals (Fe, Ni, Cu) being precipitated as respective hydroxides and hydrated oxides (so-called hydrate precipitates of nitration). For the final PGM nitration products it is shown that their co-precipitation with hydrate precipitates can result in the loss of a part of precious metals [1-3]. At the same time, iridium kinetic inertness contributes to the slow replacement of chloro ligands by nitrite ones even at elevated temperatures, while mixed-ligand iridium chloronitro complexes long dominate in solution during nitration [4, 5]. This is additionally complicated by the extreme kinetic inertness of some mixed-ligand forms, which seems to be due to *trans*-effects, as shown for *trans*- $[\text{Ir}(\text{NO}_2)_4\text{Cl}_2]^{3-}$ [6]. Captures of these PGM forms of different structures by hydrate precipitates have practically

¹Nikolaev Institute of Inorganic Chemistry, Siberian Branch, Russian Academy of Sciences, Novosibirsk, Russia; **vasilchenko@niic.nsc.ru. ²Novosibirsk State University, Novosibirsk, Russia. Original article submitted April 14, 2023; revised May 11, 2023; accepted May 11, 2023.

* Supplementary materials are available for this article at doi 10.1134/S0022476623070132 and are accessible for authorized users.

been undescribed in the literature. The main difficulties in this are the absence of reliable procedures for preparing mixed-ligand complexes and lack of information about them.

It was previously shown [7, 8] that *fac*-[Ir(NO₂)₃(L)₃] complexes, including chloronitro complexes, can be obtained by substitution of water in *fac*-[Ir(NO₂)₃(H₂O)₃]. A high lability of this aqua complex is explained by the strong *trans*-effect of nitro ligands and makes it possible to carry out substitution reactions under mild conditions. In this work, we used the exclusive reactivity of *fac*-[Ir(NO₂)₃(H₂O)₃] to prepare K₃[Ir(NO₂)₃Cl₃]·H₂O salt containing iridium trichlorotrinitro complex of the facial structure. We present the results of studying this compound by spectral techniques and the crystal structure of the compound determined by single crystal X-ray diffraction (XRD).

EXPERIMENTAL

As the starting compound for the synthesis of iridium complexes we used hydrated iridium trichloride (Krasnoyarsk Plant of Non-Ferrous Metals, 54 wt.% iridium), from which Na₃[Ir(NO₂)₆] was obtained by hydrothermal treatment in an autoclave with a NaNO₂ solution described in [6]. To nitrate iridium chloride we applied NaNO₂ (cp grade). Water-insoluble salt (NH₄)₃[Ir(NO₂)₆] was obtained by mixing Na₃[Ir(NO₂)₆] and NH₄Cl solutions according to the procedure from [9]. Nickel hydroxide for the sorption experiment was prepared by precipitation from the aqueous nickel nitrate solution (cp grade).

Preparation of *fac*-[Ir(H₂O)₃(NO₂)₃] solutions. A portion of the (NH₄)₃[Ir(NO₂)₆] salt (502 mg) was suspended in 6.25 mL of 0.3 M HNO₃ in a thick-wall glass autoclave with a Teflon screw plug with a rubber seal. The closed autoclave was heated for 1 h at 130 °C in an oil bath. After cooling the obtained solution was directly used for the synthesis. According to ¹⁵N NMR data, the fraction of *fac*-[Ir(H₂O)₃(NO₂)₃] (relative to all iridium forms) was no less than 95% in this solution [8].

Preparation of K₃[Ir(NO₂)₃Cl₃]·H₂O. An excess of KCl (1:15) was added to an aliquot of the *fac*-[Ir(H₂O)₃(NO₂)₃] solution (obtained by the mentioned procedure) containing 1.5·10⁻⁴ mol of iridium. The prepared solution was heated at 60 °C until the complete evaporation of the liquid. Then 5 mL of water were added and the solution was again evaporated. Evaporation was repeated three times, after which the obtained mixture was dissolved in 5 mL of water and the solution was evaporated to a volume of 2 mL. After cooling the solution, the *fac*-K₃[Ir(NO₂)₃Cl₃]·H₂O precipitate formed was isolated by filtration on a Teflon filter (0.22 μm), washed with a minimum amount of ice water, ethanol and dried in the air flow. The yield was 54%.

IR: ρ_w(NO₂) 640 cm⁻¹; δ(ONO) 839 cm⁻¹; ν(NO₂) 1317-1375 cm⁻¹.

UV-Vis. Electronic absorption spectra of the solutions were recorded at room temperature (23±1 °C) on a SF-102 spectrophotometer in quartz cuvettes with a 1 cm path length.

Vibrational spectroscopy. IR spectra of the salt in KBr pellets were measured on a FT-801 (Simex) spectrometer. Raman spectra were recorded on a LabRAM HR Evolution (Horiba) spectrometer with embedded argon (Ar⁺) laser excitation at a wavelength of 514 nm (0.2 mW).

TGA. The thermogravimetric analysis (TGA) was carried out on a TG 209 F3 Tarsus® NETZSCH apparatus in the helium atmosphere at gas flow rate of 30 mL/min. We used Al₂O₃ crucibles with a heating rate of 10 deg/min. The experimental data were processed using the standard Proteus analysis program package [10].

NMR. ¹⁵N NMR spectra were measured on a Bruker AVANCE 500 (AV500) spectrometer at room temperature. The ammonium nitrate solution was used as the standard.

Powder XRD. The powder XRD analysis of polycrystalline samples was performed on a Bruker D8 Advance diffractometer with a linear energy-discriminating LynxEye XE T detector at room temperature with CuK_α radiation (dynamic primary slit with a divergence of 9 mm, 3.0 mm knife collimator, 2.5° Soller slits, 0.5 s⁻¹ substrate rotation) in the Bragg–Brentano geometry. The sample was deposited on a polycarbonate substrate as a ~0.1 mm layer of the suspension in

TABLE 1. Crystallographic Characteristics and XRD Experiment Parameters

Stoichiometric formula	$\text{Cl}_3\text{H}_2\text{IrK}_3\text{N}_3\text{O}_7$
Molecular weight, g/mol	571.90
Crystal dimensions, mm	0.29×0.07×0.05
Space group	$P2_1/c$
Z	4
$a, b, c, \text{Å}$	7.3460(3), 12.9904(5), 13.1841(6)
β , deg	93.924(1)
$V, \text{Å}^3$	1255.18(9)
$\rho_{\text{cal}}, \text{g/cm}^3$	3.026
Absorption coefficient, mm^{-1}	12.292
$F(000)$	1056
θ range of data collection, deg	5.558-55.11
h, k, l index ranges	$-9 \leq h \leq 9, -16 \leq k \leq 16, -17 \leq l \leq 17$
Number of reflections measured / independent	10682 / 2902
R_{int}	0.0339
Refinement technique	Full-matrix LSM on F^2
Number of reflections / restraints / parameters	2902 / 0 / 151
S -factor on F^2	1.057
R -factor ($I > 2\sigma(I)$)	$R_1 = 0.0200, wR_2 = 0.0439$
R -factor (all data)	$R_1 = 0.0225, wR_2 = 0.0448$
$\Delta\rho_{\text{max}}, \Delta\rho_{\text{min}}, \text{e/Å}^3$	0.79, -0.88
CCDC No.	2255760

heptane. The XRD pattern was recorded in the 2θ angle range of $3\text{--}70^\circ$ with an integration step of 0.01° and the total point acquisition time of 19 s.

Single crystal XRD analysis. The XRD experiment for the $\text{K}_3[\text{Ir}(\text{NO}_2)_3\text{Cl}_3]\cdot\text{H}_2\text{O}$ salt crystals was carried out at 293 K on a four-circle Bruker Nonius X8 Apex CCD diffractometer equipped with an area CCD detector, Mo radiation, and a graphite monochromator. The structure was solved by a direct method and refined in the anisotropic-isotropic (for H) approximation. Reflection intensities were measured by ω - and ϕ -scanning of narrow (0.5°) frames. Absorption correction was applied using the SADABS program [11]. The structure was solved using SHELXT [12] and SHELXL [13] programs.

Crystallographic characteristics of $\text{K}_3[\text{Ir}(\text{NO}_2)_3\text{Cl}_3]\cdot\text{H}_2\text{O}$ salt and XRD experiment parameters are summarized in Table 1.

RESULTS AND DISCUSSION

The starting compound in the synthesis of the trichlorotrinitro complex was a solution of the *fac*- $[\text{Ir}(\text{NO}_2)_3(\text{H}_2\text{O})_3]$ molecular complex obtained by acid-induced hydrolysis of $(\text{NH}_4)_3[\text{Ir}(\text{NO}_2)_6]$ salt under hydrothermal conditions. As noted before, the lability of aqua ligands in the *fac*- $[\text{Ir}(\text{NO}_2)_3(\text{H}_2\text{O})_3]$ complex enables their easy substitution with the formation of various mixed-ligand iridium nitro complexes. In this case, the heating of the solution with an excess of potassium chloride leads to chloride ion substitution for aqua ligands. The $\text{K}_3[\text{Ir}(\text{NO}_2)_3\text{Cl}_3]\cdot\text{H}_2\text{O}$ salt formed is well soluble in water (23.8 g/L). Along with two signals corresponding to the $\text{NO}_2\text{--Ir--Cl}$ coordinate, the ^{15}N NMR spectrum of the mother liquor (Fig. 1) demonstrates a signal corresponding to the $\text{NO}_2\text{--Ir--OH}_2$ coordinate. The analysis of the integrated intensity of the signals allows the interpretation of the observed spectrum as a superposition of signals of $[\text{Ir}(\text{NO}_2)_3\text{Cl}_3]^{3-}$ and $[\text{Ir}(\text{H}_2\text{O})(\text{NO}_2)_3\text{Cl}_2]^{2-}$ complexes. The mentioned factors result in a low yield of the product (54%).

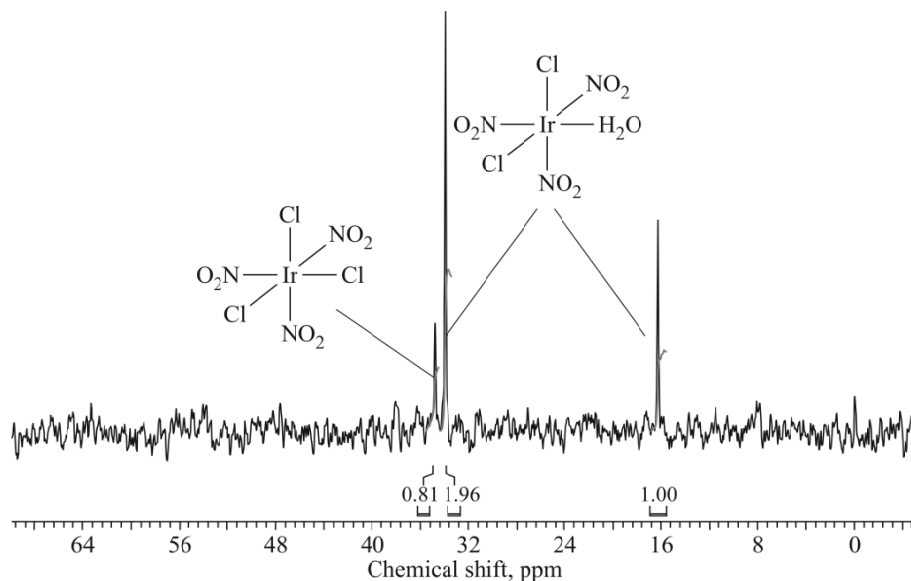


Fig. 1. ^{15}N NMR spectrum of the mother liquor of $\text{K}_3[\text{Ir}(\text{NO}_2)_3\text{Cl}_3]\cdot\text{H}_2\text{O}$ salt after the isolation of the product. ^{15}N isotope enrichment is 30%. Integrated intensities of signals in the spectrum are given together with the assignment of signals in the spectrum to assumed structures of the compounds.

Pale-yellow salt crystals (fig. S1, Supplementary materials) have a trigonal prismatic shape. The compound crystallizes in the monoclinic space group $P2_1/c$ with four formula units in the cell. The XRD pattern of the polycrystalline powder of the product isolated in the synthesis is well consistent with the XRD pattern calculated from the structural data for $\text{K}_3[\text{Ir}(\text{NO}_2)_3\text{Cl}_3]\cdot\text{H}_2\text{O}$ salt, which indicates that the obtained product is single-phase (fig. S2, Supplementary materials). The geometry of the complex $[\text{Ir}(\text{NO}_2)_3\text{Cl}_3]^{3-}$ anion in the structure is a distorted octahedron with the facial arrangement of three nitro and three chlorido ligands (Fig. 2a). The N–Ir–N angles are close to 90° ; deviations do not exceed 1° . At the same time, large scattering of values (from 87.92° to 88.94°) is observed for Cl–Ir–Cl angles, which is most likely to be due to the effect of bulky nitro ligands.

The lengths of Ir–N bonds are within 2.02–2.04 Å, while Ir–Cl are 2.37–2.38 Å. These values are similar to those observed in the respective homoleptic anions. For instance, in the $\text{Na}_3[\text{Ir}(\text{NO}_2)_6]$ structure (COD: 1536832) the Ir–N bond

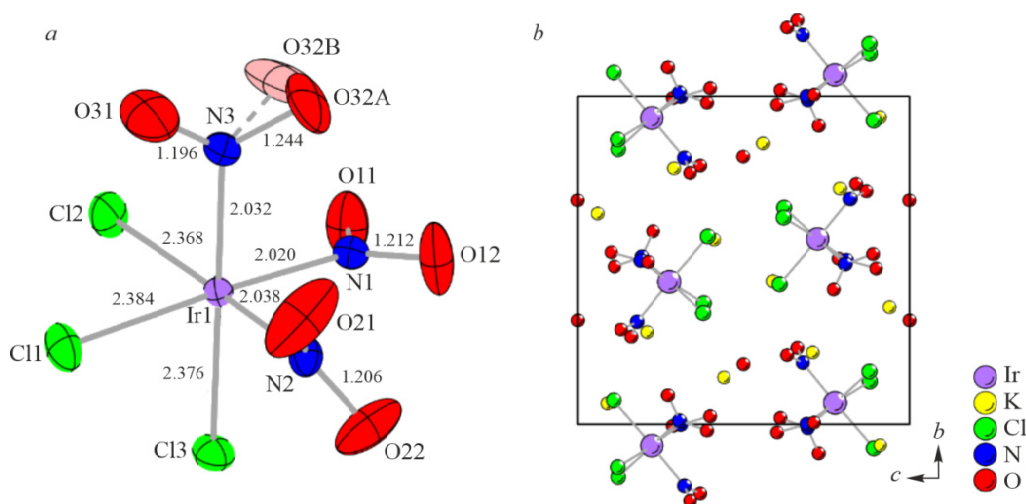


Fig. 2. Structure of the complex $[\text{Ir}(\text{NO}_2)_3\text{Cl}_3]^{3-}$ anion. Atomic thermal ellipsoids are drawn with a 50% probability (a); structure cell of the $\text{K}_3[\text{Ir}(\text{NO}_2)_3\text{Cl}_3]\cdot\text{H}_2\text{O}$ complex compound shown along the a axis (b). Hydrogen atoms are omitted.

length is 2.06 Å, whereas in $K_3[IrCl_6] \cdot H_2O$ salt [14], the shortest bond is 2.33 Å. All N–O bonds are within 1.20–1.24 Å, with disorder over the oxygen atom being observed for one of the nitro ligands. The O32 atom is found to be in two positions with the equal probability (marked as O32A and O32B). Hydrogen bonds with a water molecule can also be noted for this oxygen atom. The O–H–O contact length is 3.20 Å for the O32A position and 3.05 Å for O32B. Table 2 lists more detailed bond lengths and bond angles of the complex $[Ir(NO_2)_3Cl_3]^{3-}$ anion.

In the cell, the complex $[Ir(NO_2)_3Cl_3]^{3-}$ anions are arranged in layers along the planes perpendicular to the *c* axis. Three crystallographically independent K^+ cations (K1, K2, K3) are distinguished in the structure. The nearest environment of each complex anion contains six potassium cations at a distance from the central atom ranging from 4.11 Å to 4.52 Å (network of the shortest distances embracing all potassium and iridium atoms). There is one $[Ir(NO_2)_3Cl_3]^{3-}$ anion in the nearest environment of K1 cations, two complex anions in the environment of K2 cations, while the K3 cation is surrounded by three anions. The coordination environment of potassium cations (c.n. = 8 for all cations) is composed of oxygen atoms (K–O from 2.7 Å) and chloride ligands (K–Cl from 3.2 Å) from the composition of $[Ir(NO_2)_3Cl_3]^{3-}$ anions as well as oxygen atoms of crystal water for K1 and K2 anions.

The IR spectrum (Fig. 3(I)) of the salt in the wavenumber range of 4000–800 cm^{-1} demonstrates intense bands corresponding to stretching and rotational vibrations of crystal water (3560 cm^{-1} , 1612 cm^{-1}) and nitro ligands (1317–1375 cm^{-1} , 839 cm^{-1} , 640 cm^{-1}). Similar bands are also observed in the Raman spectrum of the compound (Fig. 3(2)). In the long-wave range of the Raman spectrum there are the absorption bands corresponding to metal–ligand stretching vibrations. The comparison of this spectrum with the spectrum of $Na_3[Ir(NO_2)_6]$ salt (Fig. S3, Supplementary materials) allows us to assign the bands at 358 cm^{-1} and 372 cm^{-1} to Ir–Cl vibrations, while the signals near 326 cm^{-1} can be assigned to Ir–N stretching vibrations. It should be noted that the position of the $\nu(Ir-Cl)$ band is close to that observed for $[IrCl_2(py)_4]Cl$ salts [15].

According to the TGA data (Fig. 4a), thermal decomposition of the salt begins at 70 °C, and first of all, results in the removal of crystal water molecules. Further decomposition consists of one stage, is accompanied by the loss of three nitro ligands, and leads to the formation of final products: iridium oxide IrO_2 and KCl (theoretical residual weight 80.86%). Weight losses in the TGA curve agree with the mass spectrometric data for gases released during thermolysis (Fig. 4b): the first step of decomposition is accompanied by water release to the gas phase; on the second step, NO is released at about 400 °C.

The UV-vis spectrum of the aqueous solution of $K_3[Ir(NO_2)_3Cl_3] \cdot H_2O$ salt (Fig. 5) exhibits a broad shoulder at 280 nm, which is located at the edge of an intense absorption band related to electronic transitions in the nitro ligand. The

TABLE 2. Selected Bond Lengths and Angles of the Structure of the $K_3[Ir(NO_2)_3Cl_3] \cdot H_2O$ Compound

Bond	Length, Å	Angle	Value, deg	Angle	Value, deg
Ir1–Cl3	2.376(9)	Cl3–Ir1–Cl1	87.92(3)	N3–Ir1–Cl1	93.8(1)
Ir1–Cl2	2.368(1)	Cl2–Ir1–Cl3	88.94(4)	N3–Ir1–N2	90.5(1)
Ir1–Cl1	2.384(1)	Cl2–Ir1–Cl1	88.04(4)	O12–N1–Ir1	120.8(2)
Ir1–N1	2.021(3)	N1–Ir1–Cl3	88.81(9)	O12–N1–O11	118.1(3)
Ir1–N2	2.038(3)	N1–Ir1–Cl2	92.38(9)	O11–N1–Ir1	121.1(3)
Ir1–N3	2.032(3)	N1–Ir1–Cl1	176.69(9)	O22–N2–Ir1	123.0(3)
N1–O12	1.211(4)	N1–Ir1–N2	90.9(1)	O22–N2–O21	117.7(4)
N1–O11	1.230(4)	N1–Ir1–N3	89.5(1)	O21–N2–Ir1	119.0(3)
N2–O22	1.206(4)	N2–Ir1–Cl3	92.52(9)	O31–N3–Ir1	122.4(3)
N2–O21	1.210(4)	N2–Ir1–Cl2	176.48(9)	O31–N3–O32B	115.1(8)
N3–O31	1.196(5)	N2–Ir1–Cl1	88.81(9)	O31–N3–O32A	115.8(8)
N3–O32B	1.21(1)	N3–Ir1–Cl3	176.5(1)	O32B–N3–Ir1	118.1(7)
N3–O32A	1.24(1)	N3–Ir1–Cl2	88.1(1)	O32A–N3–Ir1	119.9(7)

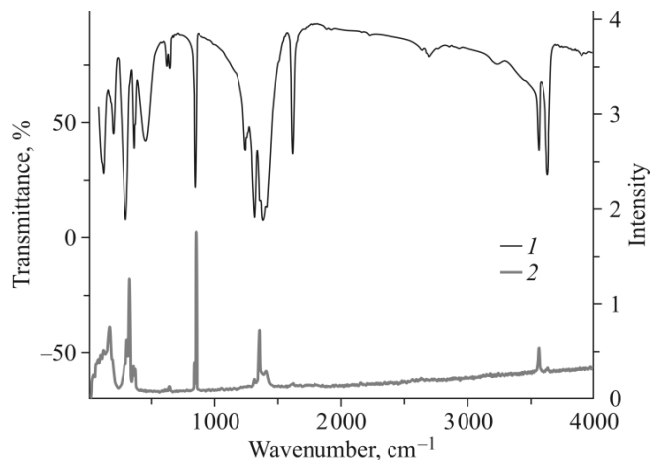


Fig. 3. IR spectrum (1) and Raman spectrum (2) of $K_3[Ir(NO_2)_3Cl_3] \cdot H_2O$ salt.

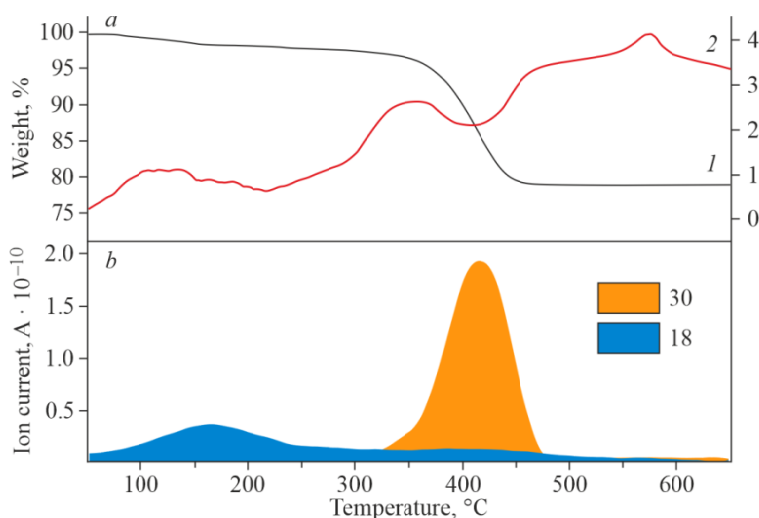


Fig. 4. TG-MS analysis of *fac*- $[Ir(NO_2)_3Cl_3]$: weight loss curve (1) and DSC (2) (a), mass spectrum of decomposition products -curves for ions with m/z values of 18 (H_2O^+) and 30 (NO^+) (b) are shown.

comparison of the spectra of related compounds ($Na_3[Ir(NO_2)_6]$, $[Ir(H_2O)_3(NO_2)_3]$) gives reason to assume that this shoulder is a superposition of two absorption bands corresponding to charge transfer from the iridium cation to chloride and nitrite ligand.

As mentioned in the introduction, the study of sorption of iridium chloronitro complexes—intermediate products of nitration of hexachloroiridate - on precipitates of basic metal hydroxides (“hydrate precipitates”) is of special interest from the practical standpoint. To evaluate sorption of the iridium(III) trichloronitro complex by “hydrate precipitates” an isothermal experiment was carried out with nickel(II) hydroxide as the model. Portions of freshly prepared nickel hydroxide were added to aliquots of the complex salt solution ($C_{Ir} = 3 \cdot 10^{-4}$ M) in water. After keeping the obtained suspensions for 10 min (23 ± 1 °C), they were centrifuged and UV-Vis spectra of the supernatant were measured. When calculating the iridium concentration after sorption, we took into account (subtracted) residual absorption seen in spectra *f* and *g* (Fig. 6a) as a shoulder extending to the visible range from the highly intense absorption edge (250 nm, OH^- anion absorption). This residual absorption seems to be due to light scattering on residual poorly filtrated nickel hydroxide particles (nanoparticles).

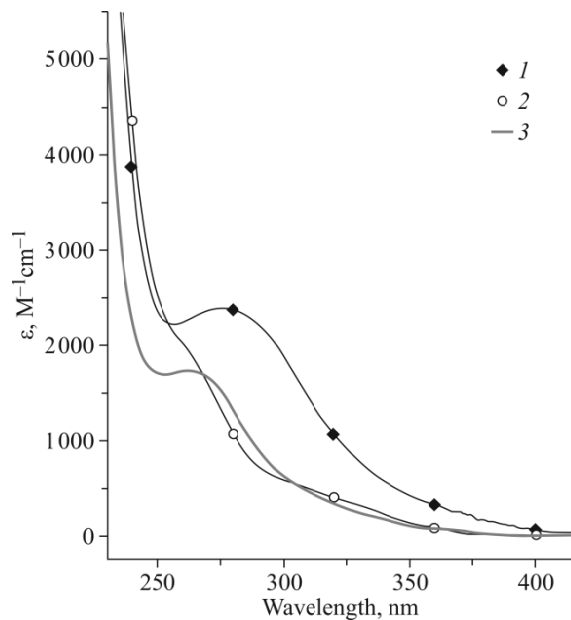


Fig. 5. UV-Vis spectra of aqueous solutions of $K_3[Ir(NO_2)_3Cl_3]$ (1), $Na_3[Ir(NO_2)_6]$ (2), $[Ir(H_2O)_3(NO_2)_3]$ (3).

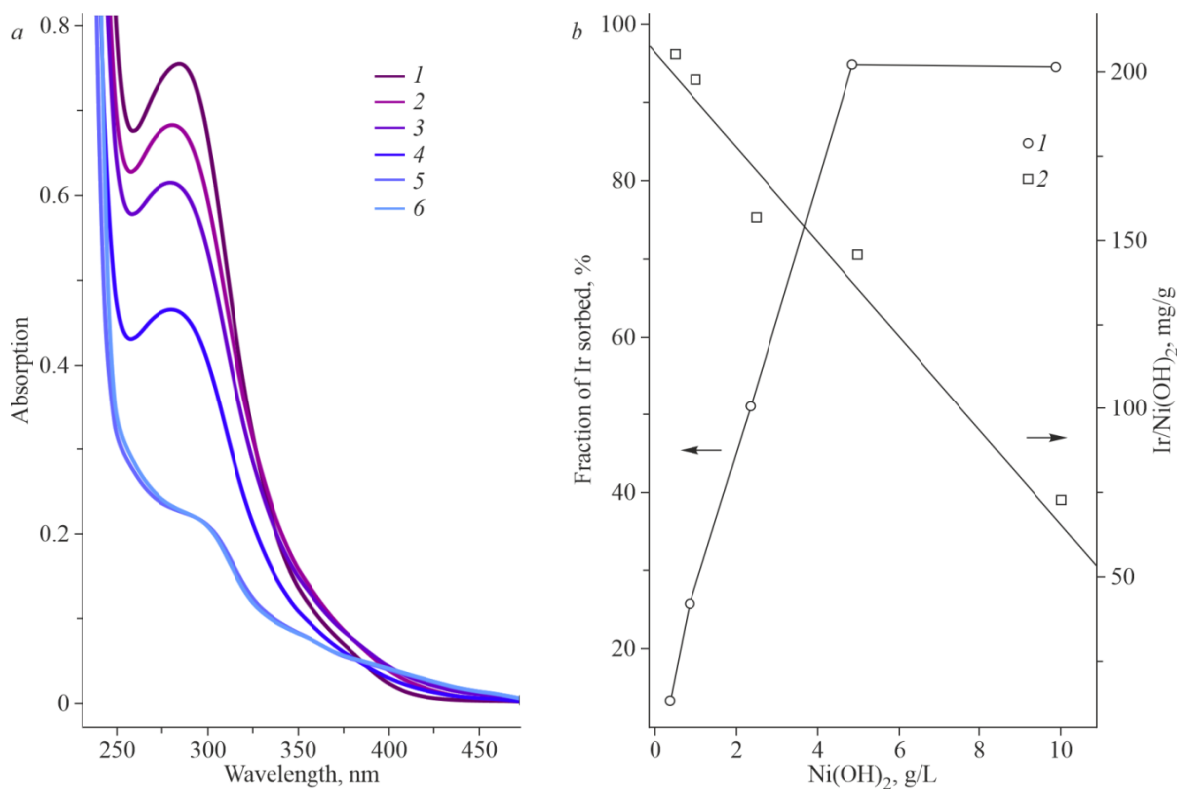


Fig. 6. UV-Vis spectrum of the solution of $K_3[Ir(NO_2)_3Cl_3] \cdot H_2O$ salt after the addition of nickel hydroxide to concentrations of 0 (initial solution), 0.5 g/L, 1 g/L, 2 g/L, 5 g/L, and 10 g/L (1-6, a); curves reflecting the amount of iridium sorbed from the $K_3[Ir(NO_2)_3Cl_3] \cdot H_2O$ solution by nickel hydroxide (1) and the specific weight concentration of iridium on it (2) (from data a) (b).

As seen from Fig. 6, after the addition of nickel hydroxide the 280 nm absorption band (shoulder) intensity decreases, with the decrease being proportional to the amount of added nickel hydroxide. When the hydroxide concentration

reaches 5 g/L, the sorption curve becomes a plateau, which corresponds to the practically complete disappearance of the absorption band. This behavior indicates the rapid sorption of the iridium complex by nickel hydroxide, while the sorption capacity estimate varies near 200 mg/g. Thus, iridium losses in hydrate precipitates can be tens of grams per precipitate kilogram because of this mechanism.

CONCLUSIONS

The synthesis and study of *fac*-K₃[Ir(NO₂)₃Cl₃]·H₂O salt are presented. A solution of the *fac*-[Ir(NO₂)₃(H₂O)₃] molecular complex was used as a source of the *fac*-{Ir(NO₂)₃} coordination synthon, which was previously noted as a convenient starting compound to obtain mixed-ligand iridium complexes with this coordination core. The main interest in iridium chloronitro complexes is associated with their role in the refining of this metal. In particular, in this work, we report the first results of studying sorption of [Ir(NO₂)₃Cl₃]³⁻ by nickel hydroxide, which models the possible mechanism of iridium losses in the industrial cycle. Further more detailed exploration of this process will help understand its kinetic nuances and expand the number of objects to other iridium chloronitro complexes.

FUNDING

The work was supported by the Ministry of Science and Higher Education of the Russian Federation, project No. 121031700315-2.

ACKNOWLEDGMENTS

The authors are grateful to S. V. Tkachev for recording NMR spectra, to Dr. P. E. Plyusnin for performing TGA, to Prof. B. A. Kolesov for providing Raman spectroscopic results, and to the Multi-Access Center of the Nikolaev Institute of Inorganic Chemistry, Siberian Branch, Russian Academy of Sciences for providing the XRD data.

CONFLICT OF INTERESTS

The authors declare that they have no conflicts of interests.

REFERENCES

1. O. N. Vyazovoi. Razrabotka tekhnologii izvlecheniya metallov platinovoi gruppy iz gidroksidov nitrovaniya affinazhnogo proizvodstva (Development of Technology for the Extraction of Platinum Group Metals from Nitration Hydroxides of Refining Production). Cand. (Chem.) Dissertation. Irkutsk: Irkutskii gosudarstvennyi tekhnicheskii universitet, **2010**. [In Russian]
2. N. V. Belousova, F. A. Kylasov, N. V. Grizan, and D. A. Solokhov. Povedenie komponentov rastvorov finishnoi ochistki affinazhnogo proizvodstva v avtoklavnykh usloviyakh (Behavior of Components of Waste Solutions of Precious Metals Refinery in Autoclave Conditions). *Zh. Sib. Fed. Univ. Ser.: Tekh. Tekhnol.*, **2015**, 8(4), 514-518, <https://sciup.org/146114977>. [In Russian]
3. N. V. Belousova, O. V. Belousov, R. V. Borisov, A. M. Kolotushkin, and P. A. Kylasov. Osazhdenie metallov platinovoi gruppy iz rastvorov affinazhnogo proizvodstva (Precipitation of Platinum Group Metals from Solutions of Precious Metals Refinery). *Zh. Sib. Fed. Univ. Khim.*, **2016**, 9(1), 6-12. <https://doi.org/10.17516/1998-2836-2016-9-1-6-12> [In Russian]
4. Handbook of Extractive Metallurgy / Ed. F. Habasbi. Wiley, **1997**.

5. F. K. Crundwell, M. S. Moats, V. Ramachandran, T. G. Robinson, and W. G. Davenport. Extractive Metallurgy of Nickel, Cobalt and Platinum Group Metals. Elsevier, **2011**. <https://doi.org/10.1016/C2009-0-63541-8>
6. A. B. Venediktov, M. A. Fedotov, S. V. Korenev, and A. V. Belyaev. Issledovanie protsessa nitrovaniya geksahlorokompleksov iridiya metodom YaMR 15N (Investigation of the nitration process of iridium hexachlorocomplexes by 15N NMR). *Koord. Khim.*, **1989**, *15*, 556-560. [In Russian]
7. P. A. Topchiyan, D. B. Vasilchenko, S. V. Tkachev, I. A. Baydina, I. V. Korolkov, D. G. Sheven, and S. V. Korenev. Mixed-ligand iridium(III) nitro complexes with phenantroline. *J. Struct. Chem.*, **2019**, *60*(4), 640-646. <https://doi.org/10.1134/s0022476619040152>
8. P. Topchiyan, D. Vasilchenko, S. Tkachev, I. Baidina, I. Korolkov, D. Sheven, S. Berdyugin, and S. Korenev. New heteroleptic iridium(III) nitro complexes derived from fac-[Ir(NO₂)₃(H₂O)₃]. *J. Mol. Struct.*, **2019**, *1182*, 100-108. <https://doi.org/10.1016/j.molstruc.2019.01.013>
9. P. Topchiyan, D. Vasilchenko, S. Tkachev, D. Sheven, I. Eltsov, I. Asanov, N. Sidorenko, A. Saraev, E. Gerasimov, A. Kurenkova, and E. Kozlova. Highly active visible light-promoted Ir/g-C₃N₄ photocatalysts for the water oxidation reaction prepared from a halogen-free iridium precursor. *ACS Appl. Mater. Interfaces*, **2022**, *14*(31), 35600-35612. <https://doi.org/10.1021/acsami.2c07485>
10. Netzsch Proteus Thermal Analysis, Ver. 4.8.1. Bayern, Germany: Netzsch-Gerätebau, **2005**.
11. SADABS. Madison, Wisconsin, USA: Bruker AXS, **2001**.
12. G. M. Sheldrick. SHELXT - Integrated space-group and crystal-structure determination. *Acta Crystallogr., Sect. A: Found. Adv.*, **2015**, *71*(1), 3-8. <https://doi.org/10.1107/s2053273314026370>
13. G. M. Sheldrick. Crystal structure refinement with SHELXL. *Acta Crystallogr., Sect. C: Struct. Chem.*, **2015**, *71*(1), 3-8. <https://doi.org/10.1107/s2053229614024218>
14. D. Rankin, B. Penfold, and J. Fergusson. The chloro and bromo complexes of iridium(III) and iridium(IV). II. Structural chemistry of Ir^{III} complexes. *Aust. J. Chem.*, **1983**, *36*(5), 871. <https://doi.org/10.1071/ch9830871>
15. K. Nakamoto. Infrared and Raman Spectra of Inorganic and Coordination Compounds, Part B: Applications in Coordination, Organometallic, and Bioinorganic Chemistry. John Wiley & Sons, **2009**.